HIGH-ENERGY GAMMA-RAY ASTRONOMY IN THE MULTIMESSENGER ERA*

Aldo Morselli

INFN Università di Roma "Tor Vergata"
Via della Ricerca Scientifica 1, Roma, Italy

(Received November 7, 2019)

The past few years have been essential for multimessenger astrophysics, with the first detection of gravitational waves from the merging of two neutron stars and the recent announcement of a high-energy neutrino event detected by IceCube coincident in direction and time with a gamma-ray flare from a blazar detected by the Fermi gamma-ray satellite. Gravitational Wave and Neutrino sources and their electromagnetic counterparts, together with new developments in transient astronomy, are an active field where the nature of many phenomena is still unknown or debated. Furthermore, the generation of new sensitive, wide-field instrumentation across the entire electromagnetic and astroparticle spectrum (SKA, CTA, KM3NeT, ELT, Athena) is set to radically change the way we perceive the Universe. In the next decade, space and ground-based detectors will jointly explore the Universe through all its messengers.

DOI:10.5506/APhysPolB.50.2057

1. Introduction

High-energy phenomena in the cosmos, and in particular processes leading to the emission of gamma rays in the energy range of 10 MeV–100 TeV, play a very special role in the understanding of our Universe. This energy range is indeed associated with non-thermal phenomena and challenging particle acceleration processes. The Universe can be thought as a context where fundamental physics, relativistic processes, strong gravity regimes, and plasma instabilities can be explored in a way that is not possible to reproduce in our laboratories. High-energy astrophysics is indeed not an esoteric subject, but is strongly linked with our daily life. Understanding of cosmic high-energy processes has an impact on our theories and laboratories applications. The technology involved in detecting gamma rays is challenging and drives our ability to develop improved instruments for a large variety of applications [1].

* Presented at the LIX Cracow School of Theoretical Physics "Probing the Violent Universe with Multimessenger Eyes: Gravitational Waves, High-energy Neutrinos, Gamma Rays, and Cosmic Rays", Zakopane, Poland, June 14–22, 2019.

At lower energies, the range between 1 and 20 MeV is an experimentally very difficult range and remained uncovered since the time of COMPTEL. New instruments can address all astrophysics issues left open by the current generation of instruments. In particular, a good angular resolution in the energy range of 10 MeV–1 GeV is crucial to resolve patchy and complex features of diffuse sources in the Galaxy and in the Galactic Center as well as increasing the point source sensitivity. This instrument addresses scientific topics of great interest to the community, with particular emphasis on multifrequency correlation studies involving radio, optical, IR, X-ray, soft gamma-ray and TeV emission. The possibility to study not only the pair production regime but also the Compton regime with this kind of detector is currently under investigation and it is another possible very interesting breakthrough.

There is a reason why we need a satellite to study these energy ranges. In figure 1, the transparency of the atmosphere for radiation of different wavelengths is shown. The solid line shows the height at which the atmoshere becomes transparent. For energies above 20 MeV, one needs to go above the atmosphere. Only at higher energies, above hundreds of GeV, you can start to observe the Cherenkov radiation produced when a gamma ray strikes Earths upper atmosphere using ground-based telescopes.

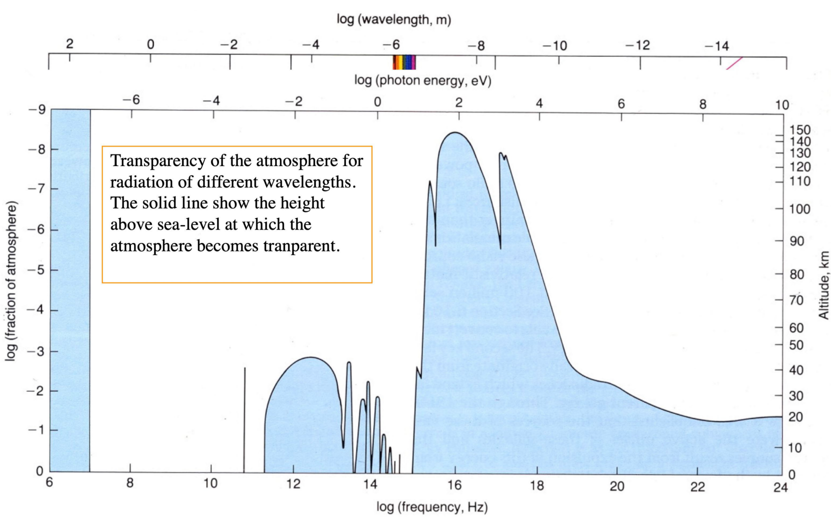

Fig. 1. Transparency of the atmosphere for radiation of different wavelenths.

The Fermi gamma-ray satellite has been in orbit since June 2008 and carries two instruments on-board: the Gamma-ray Burst Monitor (GBM) [2] and the Large Area Telescope (LAT) [3]. The GBM, sensitive in the energy range between 8 keV and 40 MeV, is designed to observe the full unocculted sky with rough directional capabilities (at the level of one to a few degrees) for the study of transient sources, particularly Gamma-ray Bursts (GRBs). LAT is the most sensitive gamma-ray detector in the 20 MeV–300GeV energy band. The LAT field of view is ∼2.4 sr then the entire sky can be observed approx. every 3 hours (2 orbits). In figure 2, the comparison between the field of view of Fermi-LAT and that of EGRET is shown and one can see that the difference is essentially due to the ratio between height and width. In the case of Fermi, the height is greatly reduced thanks to the use of silicon detectors instead of the spark chambers. The use of silicon detectors means also the lack of a consumable (spark-chamber gas) so the lifetime of the observatory can be greatly expanded.

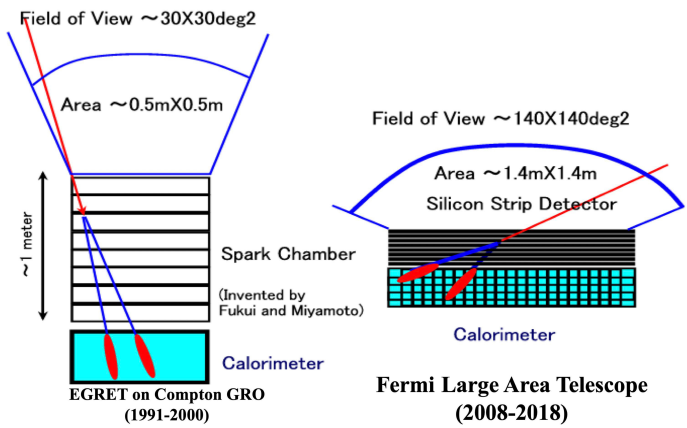

Fig. 2. Comparison between the field of view of EGRET and that of Fermi-LAT.

The operation of the instrument up to now was smooth at a level which is probably beyond the more optimistic pre-launch expectations. The LAT has been collecting science data for more than 99% of the time spent outside the South Atlantic Anomaly (SAA). The remaining tiny fractional down-time accounts for both hardware issues and detector calibrations [4, 5]. Fermi has opened a new and important window on a wide variety of phenomena, including gamma-ray observation of gravitational wave events; black holes and active galactic nuclei; gamma-ray bursts; the origin of cosmic rays and supernova remnants and searches for hypothetical new phenomena such as dark matter annihilations and Lorentz invariance violation.

2. The Fermi-LAT catalogs

The high-energy gamma-ray sky is dominated by diffuse emission: more than 70% of the photons detected by the LAT are produced in the interstellar space of our Galaxy by interactions of high-energy cosmic rays with matter and low-energy radiation fields. An additional diffuse component with an almost-isotropic distribution (and, therefore, thought to be extragalactic in origin) accounts for another significant fraction of the LAT photon sample. The rest consists of various different types of point-like or extended sources: Active Galactic Nuclei (AGN) and normal galaxies, pulsars and their relativistic wind nebulae, globular clusters, binary systems, shock-waves remaining from supernova explosions and nearby solar-system bodies like the Sun and the Moon. Figure 3 shows the all-sky counts map derived from 7 years of observation for photons with energies between 10 GeV and 2 TeV taken from the Third catalog of Hard Fermi-LAT sources (3FHL) [6].

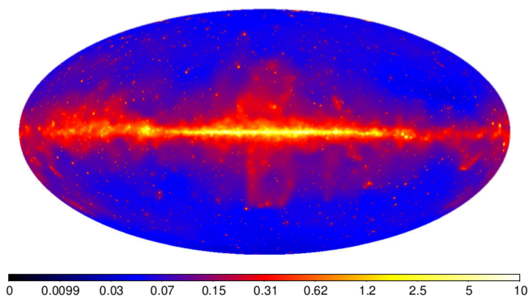

Fig. 3. Sky map of the Fermi-LAT energy flux derived from 7 years of observation. The image shows γ-ray energy flux for energies between 10 GeV and 2 TeV [6].

In figure 4, there is shown the all-sky map with the diffuse emission subtracted and with the sources divided in source class as presented in the Fermi-LAT Fourth source catalog [7].

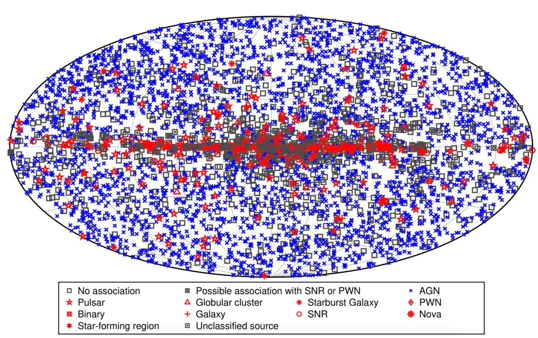

Fig. 4. Full sky map showing sources by source class. The image shows all the 5065 sources for energies between 50 MeV and 1 TeV presented in the Fermi-LAT Fourth source catalog [7] based on the first eight years of science data from the Fermi Gamma-ray Space Telescope mission.

Relative to the 3FGL catalog [7], the 4FGL catalog has twice as much exposure as well as a number of analysis improvements, including an updated model for the Galactic diffuse γ-ray emission. The 4FGL catalog includes 5065 sources above 4σ significance. 75 sources are modeled explicitly as spatially extended, and overall 354 sources are considered as identified based on angular extent, periodicity or correlated variability observed at other wavelengths. More than 3130 of the identified or associated sources are active galaxies of the blazar class, and 239 are pulsars. It is interesting that for 1337 sources, we have not found plausible counterparts at other wavelengths.

The Fermi-LAT Collaboration recently published also the second catalog of Gamma-ray Bursts [8] covering the first 10 yr of operations, from August 4, 2008 to August 4, 2018. A total of 186 GRBs are found; of these, 91 show emission in the range of 30 to 100 MeV (17 of which are seen only in this band) and 169 are detected above 100 MeV. Most of these sources were discovered by other instruments (Fermi-GBM, Swift-BAT, AGILE, INTEGRAL) or reported by the Interplanetary Network (IPN); the LAT has independently triggered on four GRBs.

Observations of GRBs with Fermi-LAT have significantly broadened our understanding of the nature of high-energy emission from these powerful transients and have led to renewed theoretical activities to model this emission.

Detection of > 10 GeV photons from GRBs has constrained models of the extragalactic background light [9] and the models leading to violation of Lorentz invariance.

The detection of the short GRB 170817A by Fermi-GBM [10] in coincidence with the gravitational wave event GW170817 [11] has proven that at least some short GRBs originate from mergers of binary neutron stars (see figure 5).

After the detection of a high energy neutrino, IceCube-170922A, with an energy of ~ 290 TeV the Fermi-LAT Collaboration realized that its arrival direction was consistent with the location of a known γ-ray blazar, TXS 0506+056, observed to be in a flaring state (see figure 6). An extensive multiwavelength campaign followed, ranging from radio frequencies to γ rays.

These observations characterize the variability and energetics of the blazar and include the detection of TXS 0506+056 in very-high-energy γ-rays. This observation of a neutrino in spatial coincidence with a γ-ray emitting blazar during an active phase suggests that blazars may be a source of high-energy neutrinos [12].

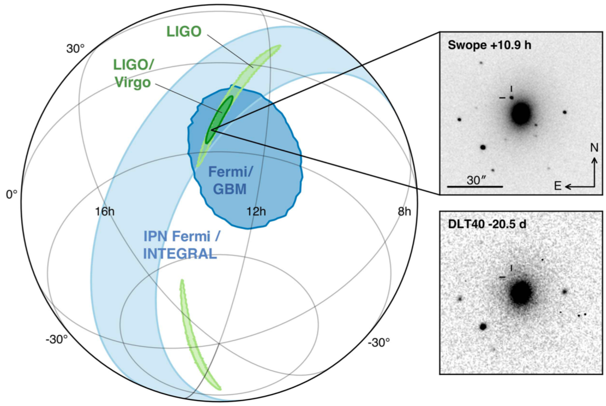

Fig. 5. (Color online) Localization of the gravitational-wave, gamma-ray, and optical signals. The left panel shows an orthographic projection of the 90% credible regions from LIGO (190 deg^2; light green), the initial LIGO-Virgo localization (31 deg^2; dark green), IPN triangulation from the time delay between Fermi and INTEGRAL (light blue), and Fermi-GBM (dark blue). The right panel shows the location of the apparent host galaxy NGC 4993 in the Swope optical discovery image at 10.9 hr after the merger (top) and the DLT40 pre-discovery image from 20.5 days prior to merger (bottom). The reticle marks the position of the transient in both images [11].

3. Indirect dark matter searches

The existence of dark matter (DM) in our Universe is well-established, but its nature is at present still unknown. Evidence indicates that the matter in the Universe cannot only consist of particles in the Standard Model (SM) of particle physics. Measurements of galactic rotation curves and galaxy cluster dynamics, measurements of the cosmic microwave background, observations of the primordial abundances of heavy isotopes produced by Big Bang nucleosynthesis, all point to a substantial fraction of the Universe's energy density being in a form of matter that does not interact signifcantly with the SM particles. Numerical simulations of large-scale structure also support this conclusion. Such simulations require non-relativistic dark matter in order to be consistent with observations. The observational evidence implies that DM is non-relativistic (cold) during the formation of large-scale structure and does not have large scattering cross sections with either itself or SM particles. No particle in the SM meets the requirements. Two favored candidates for the DM particle are weakly interactive massive particles (WIMPs, with masses in the GeV to TeV range) and axions/axion-like particles (ALPs, whose masses very poorly constrained and could range any-

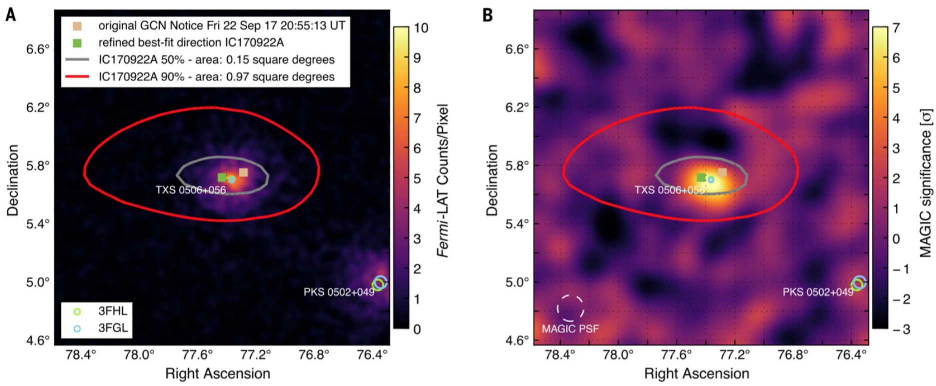

Fig. 6. (Color online) Fermi-LAT and MAGIC observations of IceCube-170922A's location. Sky position of IceCube-170922A in J2000 equatorial coordinates overlaying the γ-ray counts from Fermi-LAT above 1 GeV (A) and the signal significance as observed by MAGIC (B) in this region. The tan square indicates the position reported in the initial alert, and the green square indicates the final best-fitting position from follow-up reconstructions. Inner/gray and outer/red curves show the 50% and 90% neutrino containment regions, respectively, including statistical and systematic errors. Fermi-LAT data are shown as a photon counts map in 9.5 years of data in units of counts per pixel, using detected photons with energy of 1 to 300 GeV. MAGIC data are shown as signal significance for γ rays above 90 GeV. The locations of a γ-ray source observed by Fermi-LAT as given in the Fermi-LAT Third source catalog (3FGL) [13] and the Third catalog of Hard Fermi-LAT (3FHL) [6] source catalogs, including the identified positionally coincident 3FGL object TXS 0506+056 are also shown. For Fermi-LAT catalog objects, marker sizes indicate the 95% C.L. positional uncertainty of the source.

where from 10^{-10} to 10^{9} eV. Both types of candidates could be detected via signatures in astrophysical data (indirect-detection searches). WIMPs can self-annihilate to produce prompt or secondary gamma rays during the annihilation. If WIMPs are produced thermally in the early Universe, then the current velocity-averaged self-annihilation cross section has a natural value of $\langle\sigma_{\rm ann}v\rangle \sim 3\times10^{-26}\,{\rm cm^3s^{-1}}$. WIMP models, such as the supersymmetric neutralino, give predictions for gamma-ray energy spectra from the annihilations, which are crucial inputs, together with the DM distribution in the observed target, to estimate prospects for the sensitivity of indirect searches. The expected DM annihilation gamma-ray flux from a DM-dominated region depends on the particle physics and astrophysical (or J) factors:

$$\Phi_s(\Delta\Omega) = \frac{1}{4\pi}\frac{\langle\sigma v\rangle}{2m_{\rm DM}^2}\int_{E_{\rm min}}^{E_{\rm max}}\frac{{\rm d}N_\gamma}{{\rm d}E_\gamma}{\rm d}E_\gamma \times J(\Delta\Omega)\,, \tag{1}$$

where $\langle\sigma v\rangle$ is the velocity-averaged self-annihilation cross section, $m_{\rm DM}$ is the dark matter particle mass, $E_{\rm min}$ and $E_{\rm max}$ are the energy limits for the measurement and $\frac{{\rm d}N_\gamma}{{\rm d}E_\gamma}$ is the energy spectrum of the gammas produced in the annihilation (as, *e.g.*, from [14]). The products of DM annihilation are thought to come from decay and/or hadronization of the primary Standard Model (SM) particles: quark–antiquark, lepton and boson, and each channel is expected to have its own branching ratio. The J factor is the integral along the line of sight of the squared DM density profile of the given target integrated within an aperture angle, $\int_{\Delta\Omega}{\rm d}\Omega\int_{\rm los}\rho_{\rm DM}^2(\boldsymbol{r}){\rm d}\boldsymbol{l}$. Until recently, simulations used only cold dark matter (CDM), included only the gravitational force, and usually predicted the dark matter density to go approximately as $1/r$ towards the center of the dark matter halos. Standard parameterizations of these simulated dark matter halos are the Navarro, Frenk and White (NFW) [15] and the Einasto [16] profiles. The latter one is moderately shallower on small spatial scales compared to the NFW profile. N-body simulations showed dark matter profiles that can be both steeper and shallower. Steeper profiles are usually referred to as cuspy profiles. All the dark matter simulations agree on the main halo structure at large distances but the predictive power is limited by the spatial resolution of the simulation, and the shape and density of the profile in the inner part of the halo relies on extrapolation of the simulation prediction.

3.1. Galactic Center

The Galactic Center (GC) is expected to be the strongest source of γ rays from DM annihilation, due to its coincidence with the cusped part of the DM halo density profile [17–19] but the region is one of the richest in the gamma-ray sky. Gamma-ray emission in this direction includes the products of interactions between cosmic rays (CRs) with interstellar gas (from nucleon–nucleon inelastic collisions and electron/positron bremsstrahlung) and radiation fields (from inverse Compton scattering of electrons and positrons), as well as many individual sources such as pulsars, binary systems, and supernova remnants (SNRs). A preliminary analysis of Fermi-LAT observations of the GC region was presented in [20–22] and then analyzed in [23]. These results produced a lot of activity outside the Fermi-LAT Collaboration with claims of evidence for dark matter in the Galactic Center (*i.e.* [24, 25] and references therein). This possibility was already considered in the analysis of the EGRET galactic center excess [18] with results similar to the analysis of the Fermi-LAT data but there are other possible explanations, *e.g.*, past activity of the Galactic Center [26, 27] or a population of millisecond pulsars around the Galactic Center [28]. The Fermi-LAT Collaboration studied again the Galactic Center data in [29] with the use of 6.5 yr of data with a characterization of the uncertainty of the GC excess spectrum and morphology due to uncertainties in cosmic-ray source distributions and propagation, uncertainties in the distribution of interstellar gas in the Milky Way, and uncertainties due to a potential contribution from the Fermi bubbles with the conclusion that the nature of the GeV excess is still unclear and more studies are needed. A new experiment with better angular resolution at low energies can help to disentangle the potential contribution from other astrophysical sources (for instance, unresolved pulsars) and can help to find the cause of the effect [30, 31].

3.2. Dwarf galaxies

The dwarf spheroidal galaxies (dSphs) of the Milky Way are among the cleanest targets for indirect dark matter searches in gamma rays. They are systems with a very large mass/luminosity ratio (*i.e.*, systems which are largely DM dominated). The LAT detected no significant emission from any of such systems and the upper limits on the γ-ray flux allowed us to put very stringent constraints on the parameter space of well motivated WIMP models [32]. A combined likelihood analysis of the 10 most promising dwarf galaxies, based on 24 months of data taking and pushing the limits below the thermal WIMP cross section for low DM masses (below a few tens of GeV), has been recently performed [33]. The derived 95% C.L. upper limits

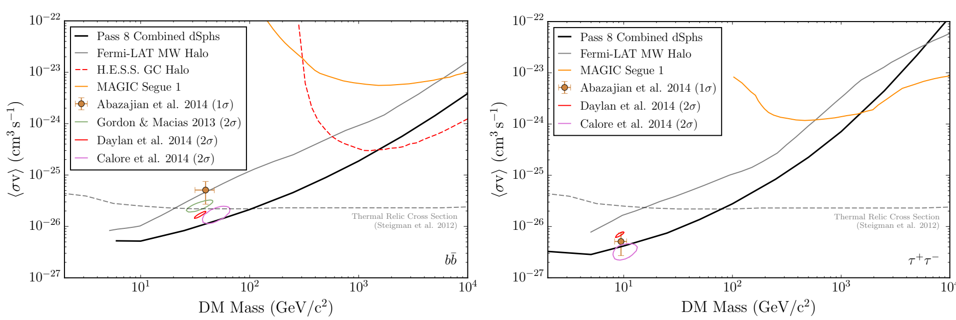

Fig. 7. Comparison of constraints on the DM annihilation cross section for the $\bar{b}b$ (left) and $\bar{\tau}\tau$ (right) channels [34] with previously published constraints from LAT analysis of the Milky Way Halo (3σ limit) [35], 112 hours of observations of the Galactic Center with H.E.S.S. [36], and 157.9 hours of observations of Segue 1 with MAGIC [37]. Closed contours and the marker with error bars show the best-fit cross section and mass from several interpretations of the Galactic Center excess [24].

on WIMP annihilation cross sections for different channels are shown in figure 7. The most generic cross section ($\sim 3 \times 10^{-26}\,\mathrm{cm}^3\,\mathrm{s}^{-1}$ for a purely s-wave cross section) is plotted as a reference. These results are obtained for NFW profiles [15], but for cored dark matter profile, the J-factors for most of the dSphs would either increase or not change much, so these results include J-factor uncertainties [33].

With the present data, we are able to rule out large parts of the parameter space where the thermal relic density is below the observed cosmological dark matter density and WIMPs are dominantly produced non-thermally, *e.g.* in models where supersymmetry breaking occurs via anomaly mediation.

4. Very-high-energy gamma-ray astronomy

Very high energy gamma-ray astronomy (VHE; $E > 100$ GeV) is a relatively young field with great scientific potential. The current generation atmospheric Cherenkov telescopes (H.E.S.S., MAGIC, and VERITAS), along with air-shower experiments (*e.g.* ARGO-YBJ, Milagro and HAWC) and with the Fermi and AGILE satellite instruments, have firmly established the field, discovering VHE radiation from more than 150 sources, comprising many source classes. A number of individual sources, both within and outside of our Galaxy, have been well-studied but there are many others that are not well-characterized or understood. It seems clear that our current knowledge represents just the tip of the iceberg in terms of the number of sources and source classes and in terms of our ability to confront the existing theoretical models. CTA will transform our understanding of the high-energy universe by discovering many hundreds of new sources, by measuring their properties with unprecedented accuracy, and also by exploring questions in physics of fundamental importance. The major scientific questions that can be addressed by CTA are the following, grouped into three broad themes:

Theme 1: Understanding the Origin and Role of Relativistic Cosmic Particles

— What are the sites of high-energy particle acceleration in the universe?

— What are the mechanisms for cosmic particle acceleration?

— What role do accelerated particles play in feedback on star formation and galaxy evolution?

Theme 2: Probing Extreme Environments

— What physical processes are at work close to neutron stars and black holes?

— What are the characteristics of relativistic jets, winds and explosions?

— How intense are radiation fields and magnetic fields in cosmic voids, and how do these evolve over cosmic time?

Theme 3: Exploring Frontiers in Physics

— What is the nature of dark matter? How is it distributed?

— Are there quantum gravitational effects on photon propagation?

— Do axion-like particles exist?

5. Core programme

The proposed CTA Key Science Projects include: *(i)* Dark Matter Programme, *(ii)* Galactic Center Survey, *(iii)* Galactic Plane Survey, *(iv)* Large Magellanic Cloud Survey, *(v)* Extragalactic Survey, *(vi)* Transients, *(vii)* Cosmic-ray PeVatrons, *(viii)* Star Forming Systems, *(ix)* Active Galactic Nuclei, and *(x)* Clusters of Galaxies. A few highlights from these projects are described here, focusing on the surveys and the search for dark matter:

The Galactic Center Survey consists primarily of a deep (525 h) exposure with pointings on a small grid centered on Sgr A*; this exposure covers the central source, the center of the dark matter halo, the primary diffuse emission and multiple supernova remnant (SNR) and pulsar wind nebula (PWN) sources. An extended survey (300 h) of a $10^\circ \times 10^\circ$ region around the Galactic Center would cover the edge of the Galactic Bulge, the base of the Fermi Bubbles, the radio spurs and the Kepler SNR.

The Dark Matter Programme is centered on the indirect search for dark matter via the weakly interacting massive particle (WIMP) annihilation signal [38]. As shown in figure 8, the deep exposure of the Galactic Center region will allow CTA to reach a sensitivity to a thermal relic WIMP over a wide mass region, thus nicely complementing searches done with the Fermi satellite, at the Large Hadron Collider and by direct-detection experiments. Additional dark matter targets include dwarf spheroidal galaxies, the LMC and the Perseus cluster. The effect of systematics is drastically reduced for dwarf spheroidal galaxies compared to the extended Galactic Halo, explaining the significant interest in observations of dwarfs.

The Galactic Plane Survey is a survey of the entire Galactic plane, with deeper exposure in the inner Galaxy and Cygnus region. The survey will be a factor of 5–20 more sensitive than previous surveys carried out at very high energies and is thus expected to sample a much larger fraction of the log N–log S distribution of Galactic sources, as

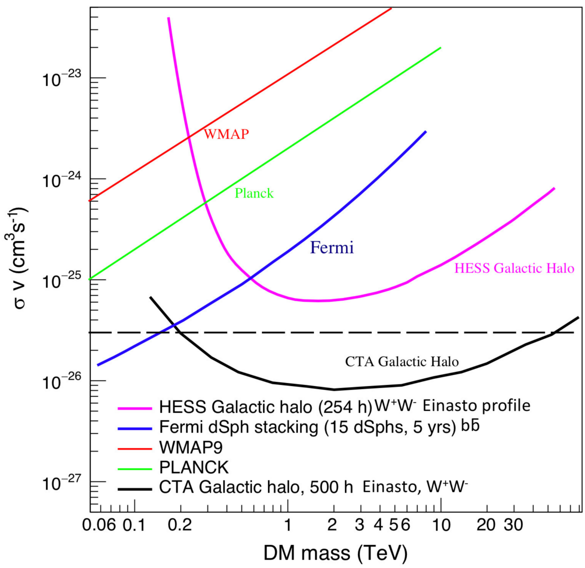

Fig. 8. Current best limits on the annihilation cross section from indirect detection (Fermi-LAT dwarf spheroidal galaxies stacking analysis, W^+W^- channel [34], H.E.S.S. Galactic Halo W^+W^- channel [39]) and cosmic microwave background (WMAP and Planck $b\bar{b}$ channel [40]) experiments compared with the projected sensitivity for CTA from observations of the Galactic Halo for the Einasto profile, W^+W^- channel. The expectation for CTA is optimistic as it includes only statistical errors. The effect of the Galactic diffuse emission can affect the results by $\sim 50\%$. The dashed line shows the thermal relic cross section [38].

shown in figure 9. The discovery of many hundreds of sources in the Galactic Plane Survey will be an important pathfinder for later GO proposals.

The Large Magellanic Cloud (LMC) Survey will cover this star-forming galaxy in its entirety, resolving regions down to 20 pc in size and with sensitivity down to a luminosity of $\sim 10^{34}$ erg/s. Long-term monitoring of SN 1987A will be carried out, provided the source is detected in the first phase of the survey.

The Extragalactic Survey will be the first wide-field (one-quarter of the sky) survey of the VHE sky at high sensitivity. Aimed to provide an unbiased sample of galaxies (particularly active Galactic nuclei, AGN), the survey will also be sensitive to unexpected phenomena at high Galactic latitudes.

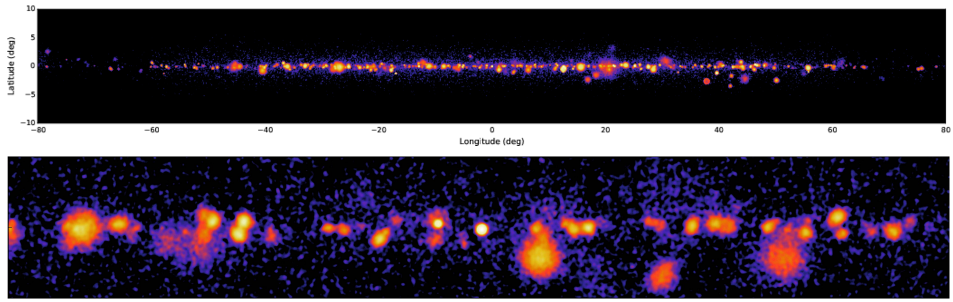

Fig. 9. Top: Simulated CTA image of the Galactic plane for the inner region, $-80° < l < 80°$, adopting the proposed Galactic Plane Survey observation strategy and a source model that contains supernova remnant and pulsar wind nebula populations as well as diffuse emission. Bottom: A close-in view of a 20° region in Galactic longitude [41].

6. CTA design: performance goals, concept, and array layouts

To achieve these broad science goals in a meaningful way, CTA must improve upon the performance of existing instruments in many areas simultaneously. The various performance goals, along with the science drivers that provide their impetus, are the following:

High sensitivity (a factor of up to ten improvement over current experiments): impacts all science topics;

Wide Energy Coverage (20 GeV to $\geq$ 300 TeV): low-energy sensitivity is needed to detect the most distant sources whose spectra are cut off from absorption on intergalactic radiation fields; very high energy reach is needed to detect PeVatron sources that would help explain the origin of cosmic rays up to the knee in the spectrum;

Full-sky Coverage (arrays in both hemispheres): enable the full characterization of the VHE universe and access to unique sources in both hemispheres;

Wide Field-of-View ($\sim$ 8 deg): permits more rapid surveys and better study of extended sources;

Excellent Resolution in angle (few arc-minutes) and energy ($\sim$10%): permits good reconstruction of source morphology and spectra;

Rapid Response ($\sim$ 30 s slewing to/from anywhere in observable sky): enables rapid follow up of transient sources.

To meet these performance goals, CTA will extend the atmospheric Cherenkov technique to its logical next level, by deploying large arrays of telescopes that cover an area on the ground that is significantly larger than the Cherenkov light pool. Compared to the existing instruments consisting of several telescopes separated by about 100 m, the larger number of telescopes and the larger area covered by CTA will result in: *(i)* a much higher rate of showers contained within the footprint of the array, *(ii)* a better sampling of the showers from different viewing angles that will greatly improve the shower reconstruction and the cosmic-ray background rejection, and *(iii)* a lower energy threshold since the central part of the shower (with the highest Cherenkov photon density) generally falls within the array. To achieve the goal of wide energy range within cost constraints leads to the logical choice of a graded array of telescopes of different sizes.

In CTA, the lowest energies are covered by four large-sized telescopes (LSTs) that are capable of detecting gamma rays down to 20 GeV. The core energy range of 100 GeV to 10 TeV is covered by an array of 25 (South) or 15 (North) medium-sized telescopes (MSTs), and, for the Southern array, the highest energies are covered by a several km^2 array of 70 small-sized telescopes (SSTs). To achieve fast-response to low-energy transients such as gamma-ray bursts, the LSTs will incorporate very rapid slewing. Conversely, to achieve a wide field-of-view for surveys and extended Galactic sources, the MSTs and SSTs will employ wide-field cameras. To realize full-sky coverage, CTA arrays will be deployed in both hemispheres. The small-sized telescopes are only planned for the Southern array because the highest energies are most relevant for the study of Galactic sources.

The layout of the telescopes in the CTA arrays has been determined over a number of years by a multi-step process starting with semi-analytic estimates and continuing with large-scale simulations that include full shower and detector modeling. The latest simulations incorporate site-dependent effects (including altitude, geomagnetic field, and telescope positioning constraints) to assess the performance attributes of CTA. Figure 10 shows the current baseline array layouts for the Southern and Northern CTA sites resulting from this optimization process.

Figure 11 shows on the left the differential energy flux sensitivities for CTA (South and North) and on the right the angular resolution expressed as the 68% containment radius of reconstructed gamma rays. Figure 12 shows on the left the energy resolution as a function of reconstructed energy for the North site and on the right for the South sites.

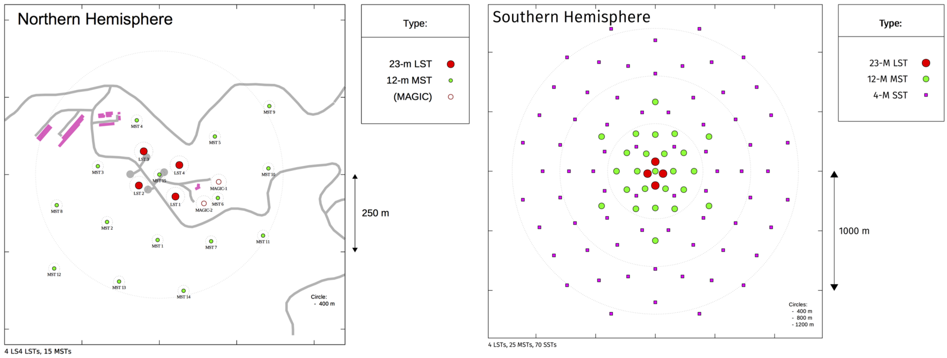

Fig. 10. (Color online) Possible layouts for the baseline arrays for CTA South (left) and CTA North (right). The LSTs are identified by the black/red circles, the MSTs by the grey/green circles, and the SSTs by the purple squares [41].

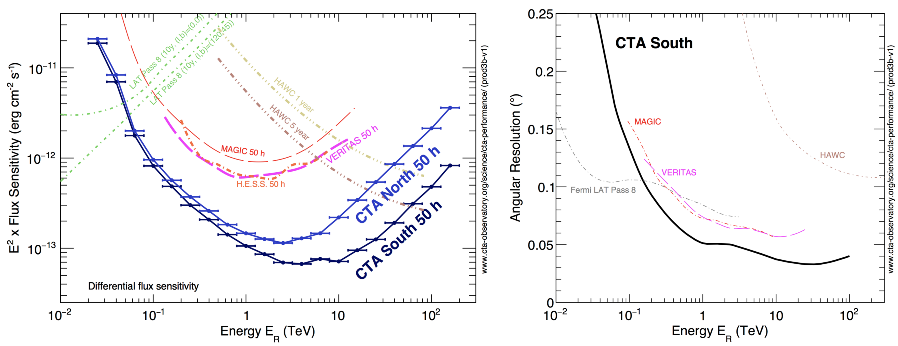

Fig. 11. Left: Differential energy flux sensitivities for CTA (south and north) and selected existing gamma-ray instruments for five standard deviation detections in five independent logarithmic bins per decade in energy. For the CTA sensitivities, additional criteria are applied to require at least ten detected gamma rays per energy bin and a signal/background ratio of at least 1/20. The curves for Fermi-LAT and HAWC are scaled by a factor of 1.2 to account for the different energy binning. The curves shown give only an indicative comparison of the sensitivity of the different instruments, as the method of calculation and the criteria applied are different. Right: Angular resolution expressed as the 68% containment radius of reconstructed gamma rays (the resolution for CTA North is similar) [41].

Figure 13 shows the effective collection area after gamma/hadron separation cuts but without any cut in the reconstructed event direction optimized for 50 h observation time for the North site (left) and the South site (right). Figure 14 shows the differential sensitivity curves for a point-like source at increasing angular distances from the center of the Field-of-View (FoV). The

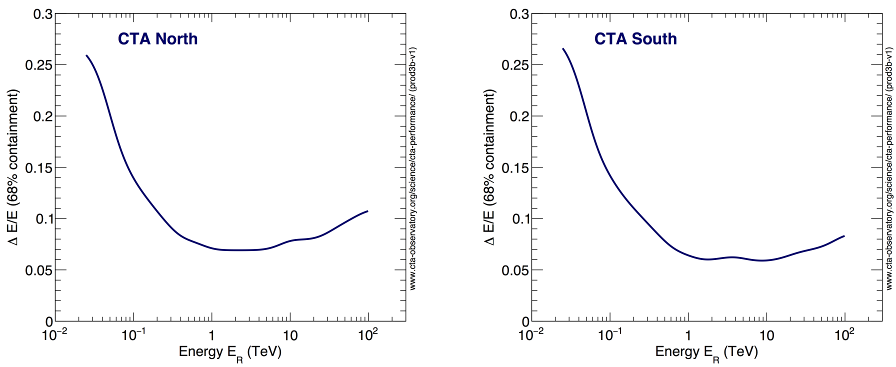

Fig. 12. Energy resolution as a function of reconstructed energy (the result depends only weakly on the assumed gamma-ray spectrum) for the North site (left) and the South site (right) [41].

radius of the FoV region in which the sensitivity is within a factor 2 of that at the center is around 2 degrees near the CTA threshold, and >3 degrees above a few 100 GeV.

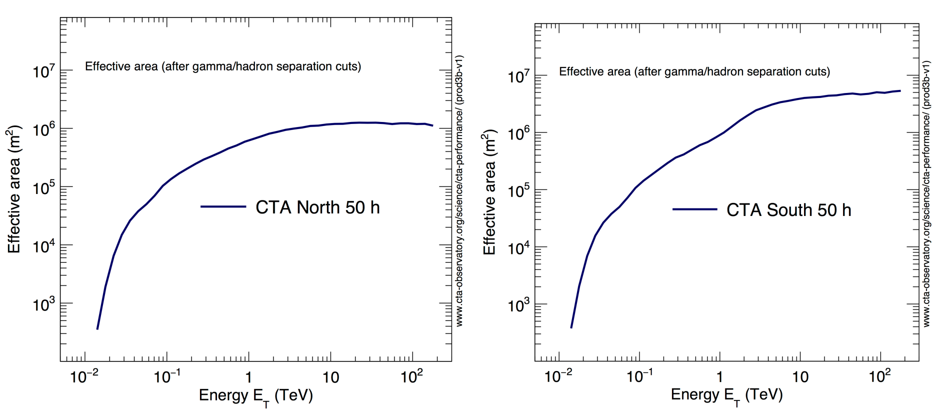

Fig. 13. Effective collection area after gamma/hadron separation cuts but without any cut in the reconstructed event direction optimized for 50 h observation time for the North site (left) and the South site (right) [41].

Figure 15 shows the differential flux sensitivity of CTA at selected energies as a function of observing time in comparison with the Fermi-LAT instrument (Pass 8 analysis, extragalactic background, standard survey observing mode). The differential flux sensitivity is defined as the minimum flux needed to obtain a 5-standard-deviation detection from a point-like gamma-ray source, calculated for energy bins of a width of 0.2 decades. An

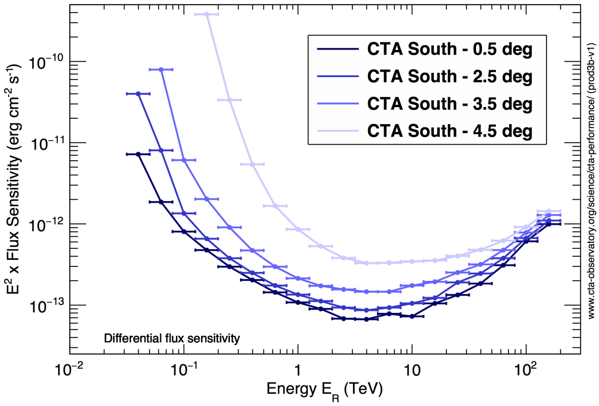

Fig. 14. Differential sensitivity curves for a point-like source at increasing angular distances from the center of the FoV [41].

additional constraint of a minimum of 10 excess counts is applied. Note that especially for exposures longer than several hours, the restrictions on observability of a transient object are much stricter for CTA than for the Fermi-LAT. CTA will be able to observe objects above 20 degrees elevation during dark sky conditions.

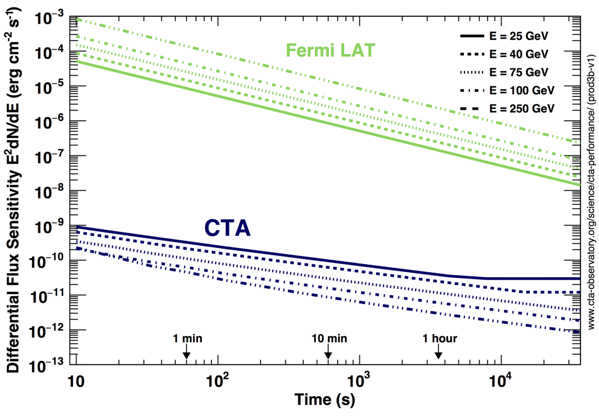

Fig. 15. Differential flux sensitivity of CTA at selected energies as a function of observing time in comparison with the Fermi-LAT instrument (Pass 8 analysis, extragalactic background, standard survey observing mode) [41].

7. Current status of CTA

CTA was conceived and is being designed by the Cherenkov Telescope Array Consortium (CTAC), a collaboration of more than 1400 scientists and engineers from 32 countries around the world. The Consortium has developed the primary science themes of CTA and Consortium Institutes are expected to provide the bulk of the CTA components, including telescopes, cameras and software. The CTA Observatory (CTAO) was established in 2014 to provide the legal entity to oversee the CTA Project Office which manages the construction of CTA. Governed by a Council of country representatives, CTAO will be responsible for observatory operations and data management. During the last several years, the progress towards realization of CTA has been accelerating. The baseline design and core technologies are now established, several prototype telescopes have been completed and are undergoing testing, the two CTA sites have been selected, and a large portion of the required funding has now been identified. Thus, the project is well-positioned for a construction start in 2018 and the turn-on of full operations by the middle of the next decade.

7.1. CTA sites

CTAO activities will be carried out at the two CTA array sites and at the CTA Headquarters (HQ) and Science Data Management Centre (SDMC). Pending successful completion of hosting agreements, the CTA HQ will be hosted at the INAF site in Bologna, Italy and the CTA SDMC will be on the DESY campus in Zeuthen, Germany. Following a lengthy process that included detailed assessment and external review, the CTA Resource Board (a precursor to the CTA Council) selected the following two sites to host CTA arrays:

South: European Southern Observatory (ESO) Paranal site in Chile;

North: Instituto de Astrofisica de Canarias (IAC) Roque de los Muchachos Observatory site in La Palma, Spain.

Activities to prepare the sites are well underway in both hemispheres. Technical and infrastructure studies are being carried out in the context of the Royal Institute of British Architects (RIBA) process. CTA is currently in the advanced design phase (RIBA-3) and is approaching the technical design phase (RIBA-4). Specific activities include power, lightning protection, geotechnical, ground investigation, and general infrastructure (roads, buildings, foundations, *etc.*) studies. At La Palma, the construction of the first prototype LST is finished and the commissioning will be finished by 2020.

7.2. Prototype telescopes

Extensive work has been carried out within the CTA Consortium over a number of years to prototype the hardware and software for all three telescope sizes. This work builds on the successes and experiences of the current generation of imaging atmospheric Cherenkov telescopes, but it also makes use of new techniques. For example, in the telescope design, both single mirror (based on the Davies–Cotton, or DC, design) and dual mirror (based on the Schwarzschild-Couder, or SC, design) approaches are being developed. For the photosensors in the cameras, both photomultiplier tubes (PMTs) and Silicon photomultipliers (Si-PMs) are being evaluated. In all camera designs, the read-out electronics (typically using 1 GS/s high-speed sampling ASICs) are contained in the focal-plane box. Figure 16 shows recent photos of the various prototypes of CTA telescopes. For the LST, the requirement of a large mirror area to reach the lowest gamma-ray energies has led to a single mirror design using a 23 m diameter parabolic reflector. This very large telescope will use PMTs. For the MST, two designs are being considered. A single mirror DC design has been developed at a site in Adlershof, Germany that makes use of a 12 m diameter dish with a focal length of 16 m and a PMT camera. Two read-out schemes are being prototyped that make use of either 250 MS/s Flash-ADCs with digital storage or 1 GS/s ASICs. A dual mirror SC MST prototype is being built at the Whipple Observatory in Arizona, USA that will employ a 9.7 m primary mirror and a compact high-resolution camera using Si-PMs. For the SST, three approaches are being considered, with each having a primary mirror size of 4 m diameter and cameras using Si-PMs. Two of these use the SC design: the SST-2M-ASTRI prototyped at Serra La Nave, Sicily, Italy and SST-2M-GCT in Meudon, France. The third SST prototype, SST-1M, is being developed in Kraków, Poland and makes use of the DC design.

8. Synergies

CTA will have important synergies with many of the new generation of astronomical and astroparticle observatories. As the flagship VHE gamma-ray observatory for the coming decades, CTA plays a similar role in the VHE waveband as the SKA in radio, ALMA at millimetre, or E-ELT/TMT/GMT in the optical wavebands, providing excellent sensitivity and resolution compared to prior facilities. At the same time, the scientific output of CTA will be enhanced by the additional capabilities provided by these instruments (and *vice versa*).

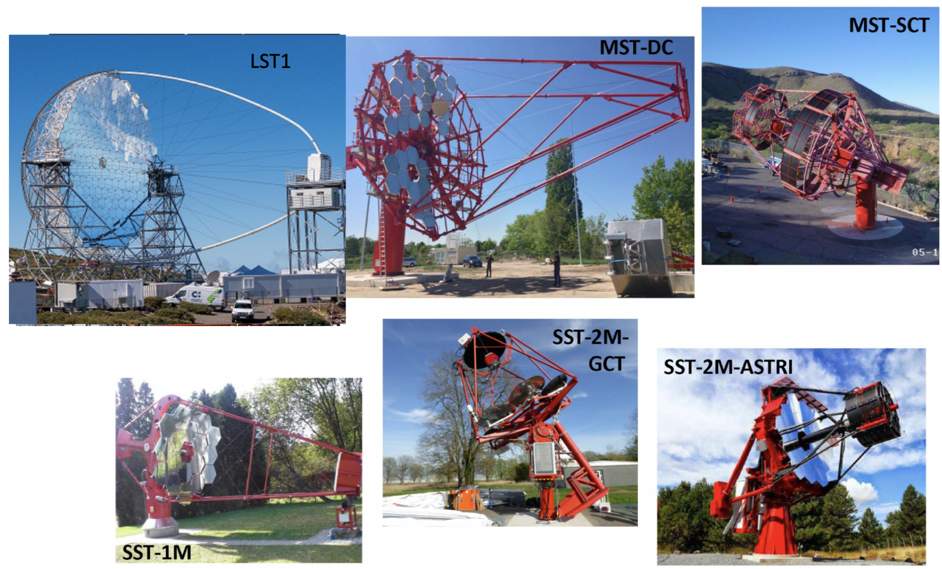

Fig. 16. Prototype telescopes being developed for CTA. Top row (left to right): LST, MST-DC in Germany, MST-SCT in USA. Bottom row (left to right): SST-1M in Poland, SST-2M-GCT in France, and SST-2M-ASTRI in Italy.

Multi-wavelength (MWL) and multimessenger (MM) studies using CTA provide added value to the science cases in two main ways:

> Non-thermal emission: To understand the origin of cosmic rays and the extreme physical environments that produce them, it is necessary to study non-thermal signatures that span many orders of magnitude in frequency in the broad-band spectral energy distribution (SED) of a given object. In the case of time-variable emission, such studies require simultaneous observations and/or alerts and triggers between observatories.

> Source properties: Information on the nature of gamma-ray emitting sources can be provided by MWL observations, enabling, for example, the object class, environmental conditions or the distance to be established. For this purpose, simultaneous observations are in general not required, except for the need to characterize transient sources, for example in the case of gamma-ray burst redshift measurements.

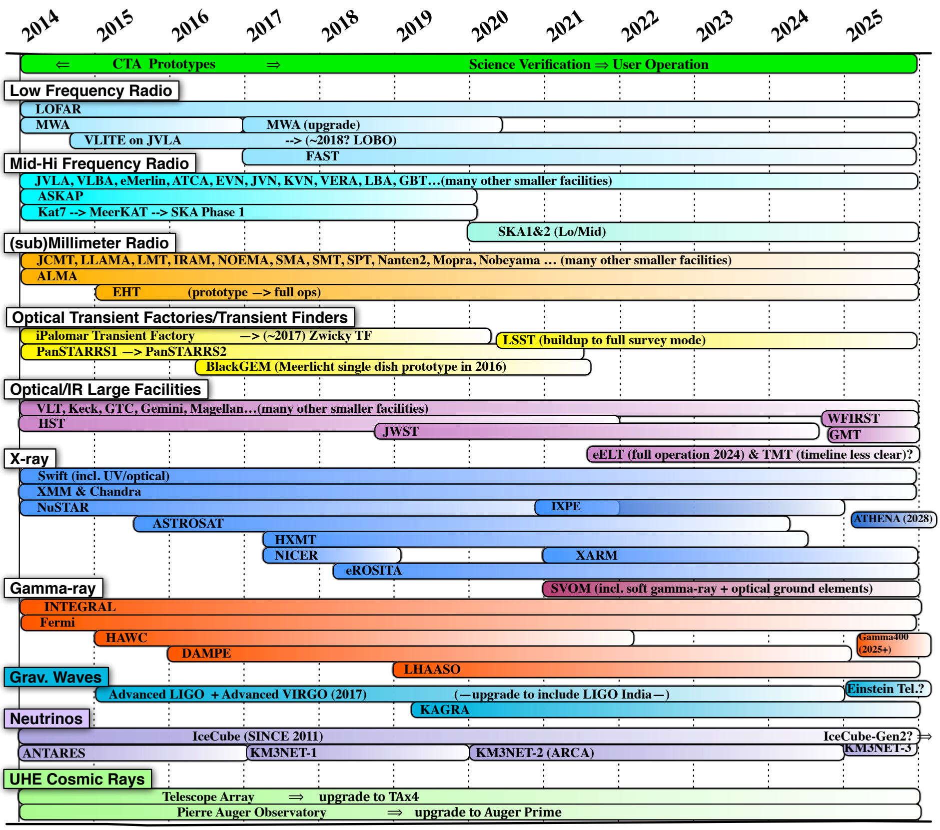

Fig. 17. Timeline of major multi-wavelength/multimessenger facilities over the next decade. Note that the lifetimes of many facilities are uncertain, contingent on performance and funding. We indicate this uncertainty via the gradient, but have chosen timelines based on the best information currently available [41].

The need for (simultaneous) MWL and MM observations has been considered as a factor in the site selection process for CTA and in the preparations for CTA science. A summary timeline of major facilities is shown in figure 17.

All these facilities will contribute together with all the indirect, direct and accelerator experiments to the study of the fundamental laws of nature and the search for dark matter in the sky, on-ground, in the water, in ice, underground and at accelerator machines, as shown in figure 18.

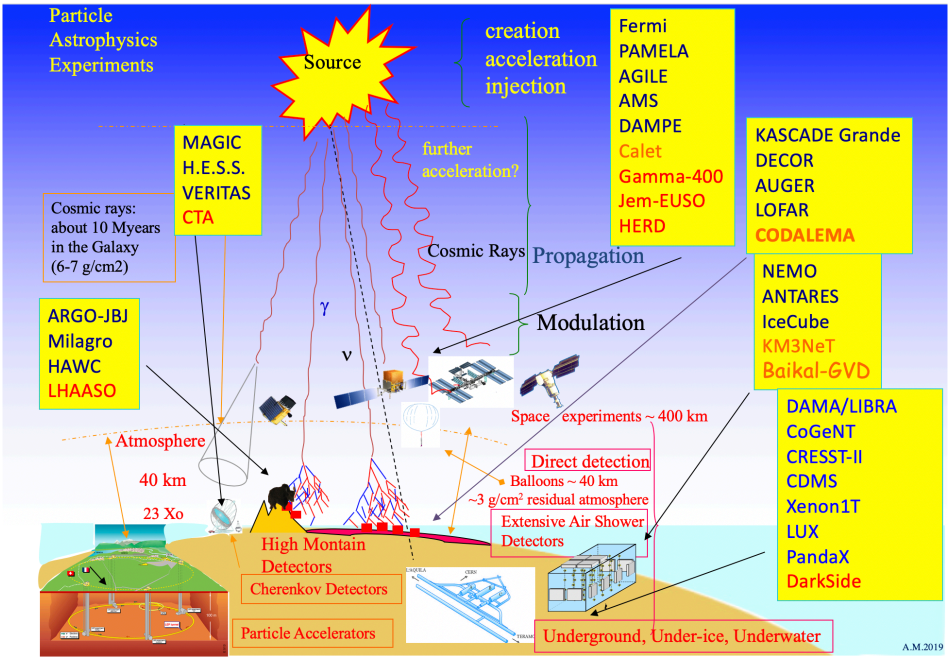

Fig. 18. (Color online) Indirect, direct and accelerator experiments for the study of the fundamental laws of nature and the search of dark matter (future experiments are in light grey/red).

The Fermi-LAT Collaboration acknowledges support from a number of agencies and institutes for both development and the operation of the LAT as well as scientific data analysis. These include NASA and DOE in the United States, CEA/Irfu and IN2P3/CNRS in France, ASI and INFN in Italy, MEXT, KEK, and JAXA in Japan, and the K.A. Wallenberg Foun- dation, the Swedish Research Council and the National Space Board in Sweden. Additional support from INAF in Italy and CNES in France for science analysis during the operations phase is also gratefully acknowledged. The CTA Consortium acknowledges financial support from the agencies and organizations listed here: `http://www.cta-observatory.org/consortium_acknowledgments` This paper has gone through internal review by the CTA Consortium.

REFERENCES

[1] A. Morselli, *Front. Phys.* **5**, 3 (2017).

[2] C. Meegan *et al.*, *AIP Conf. Proc.* **662**, 469 (2003).

[3] W.B. Atwood *et al.* [Fermi-LAT Collab.], *Astrophys. J.* **697**, 1071 (2009) [`arXiv:0902.1089 [astro-ph.HE]`].

[4] M. Ackermann *et al.* [Fermi-LAT Collab.], *Astropart. Phys.* **35**, 346 (2012) [arXiv::1108.0201 [astro-ph.IM]].

[5] M. Ackermann *et al.* [Fermi-LAT Collab.], *Astrophys. J. Suppl. Ser.* **203**, 4 (2012) [arXiv:1206.1896 [astro-ph.IM]].

[6] M. Ackermann *et al.* [Fermi-LAT Collab.], *Astrophys. J. Suppl. Ser.* **232**, 18 (2017) [arXiv:1702.00664 [astro-ph.HE]].

[7] S. Abdollahi *et al.* [Fermi-LAT Collab.], arXiv:1902.10045 [astro-ph.HE], submitted to *Astrophys. J. Suppl. Ser.*

[8] M. Ajello *et al.* [Fermi-LAT Collab.], *Astropart. Phys.* **878**, 52 (2019) [arXiv:1906.11403 [astro-ph.HE].

[9] A. Abdo *et al.* [Fermi-LAT Collab.], *Astropart. Phys.* **723**, 1082 (2010) [arXiv:1005.0996 [astro-ph.HE]].

[10] A. Goldstein *et al.* [Fermi-GBM Collab.], *Astropart. Phys. Lett.* **848**, L14 (2017).

[11] B. Abbott *et al.*, *Astropart. Phys. Lett.* **848**, L12 (2017) [arXiv:1710.05833 [astro-ph.HE]].

[12] The IceCube Collab., Fermi-LAT, MAGIC, AGILE, ASAS-SN, HAWC, H.E.S.S, INTEGRAL, Kanata, Kiso, Kapteyn, Liverpool Telescope, Subaru, Swift/NuSTAR, VERITAS, and VLA/17B-403 teams, *Science* **361**, eaat1378 (2018).

[13] F. Acero *et al.* [Fermi-LAT Collab.], *Astrophys. J. Suppl. Ser.* **218**, 23 (2015) [arXiv:1501.02003 [astro-ph.HE]].

[14] M. Cirelli *et al.*, *J. Cosmol. Astropart. Phys.* **1103**, 051 (2011) [*Erratum-ibid.* **1210**, E01 (2012)] [arXiv:1012.4515 [hep-ph]].

[15] J. Navarro, J. Frenk, S. White, *Astropart. Phys.* **46**, 563 (1996) [arXiv:astro-ph/9508025].

[16] A.W. Graham *et al.*, *Astron. J.* **132**, 2711 (2006).

[17] A. Morselli *et al.*, *Nucl. Phys. B* **113**, 213 (2002).

[18] A. Cesarini *et al.*, *Astropart. Phys.* **21**, 267 (2004) [arXiv:astro-ph/0305075].

[19] E. Baltz *et al.*, *J. Cosmol. Astropart. Phys.* **07**, 013 (2008) [arXiv:0806.2911 [astro-ph]].

[20] V. Vitale, A. Morselli [Fermi-LAT Collab.], Proceedings of the 2009 Fermi Symposium, eConf Proceedings C091122 [arXiv:0912.3828 [astro-ph.HE]].

[21] L. Goodenough, D. Hooper, arXiv:0910.2998 [hep-ph].

[22] A. Morselli, B. Cañadas, V. Vitale, *Nuovo Cim.* **34C**, 3 (2011) [arXiv:1012.2292 [astro-ph.HE]].

[23] M. Ajello *et al.* [Fermi-LAT Collab.], *Astrophys. J.* **819**, 44 (2016) [arXiv:1511.02938 [astro-ph.HE]].

[24] F. Calore *et al.*, *J. Cosmol. Astropart. Phys.* **03**, 37 (2015) [arXiv:1409.0042 [astro-ph.CO]].

[25] T. Daylan *et al.*, *Phys. Dark Univ.* **12**, 1 (2016) [arXiv:1402.6703 [astro-ph.HE]].

[26] J. Petrovic *et al.*, *J. Cosmol. Astropart. Phys.* **10**, 052 (2014) [arXiv:1405.7928 [astro-ph.HE]].

[27] E. Carlson, S. Profumo, *Phys. Rev. D* **90**, 023015 (2014).

[28] S. Lee *et al.*, *Phys. Rev. Lett.* **116**, 051103 (2016) arXiv:1506.05124 [astro-ph.HE]].

[29] M. Ackermann *et al.* [Fermi-LAT Collab.], *Astrophys. J.* **840**, 43 (2017) [arXiv:1704.03910 [astro-ph.HE]].

[30] A. De Angelis *et al.*, *J. High Energy Astrophys.* **19**, 1 (2018).

[31] A. Morselli *et al.*, *Nucl. Phys. B Proc. Suppl.* **239**, 193 (2013) [arXiv:1406.1071 [astro-ph.IM]].

[32] A. Abdo *et al.* [Fermi-LAT Collab.], *Astrophys. J.* **712**, 147 (2010) [arXiv:1001.4531 [astro-ph.CO]].

[33] M. Ackermann *et al.* [Fermi-LAT Collab.], *Phys. Rev. Lett.* **107**, 241302 (2011) [arXiv:1108.3546 [astro-ph.HE]].

[34] M. Ackermann *et al.* [Fermi-LAT Collab.], *Phys. Rev. Lett.* **115**, 231301 (2015) [arXiv:1503.02641 [astro-ph.HE]].

[35] M. Ackermann *et al.* [Fermi LAT Collab.], *Astrophys. J.* **761**, 91 (2012) [arXiv:1205.6474 [astro-ph.CO]].

[36] A. Abramowski *et al.* [H.E.S.S. Collab.], *Phys. Rev. Lett.* **106**, 161301 (2011) [arXiv:1103.3266 [astro-ph.HE]].

[37] J. Aleksić *et al.* [MAGIC Collab.], *J. Cosmol. Astropart. Phys.* **1402**, 008 (2014) [arXiv:1312.1535 [hep-ph]].

[38] A. Morselli, *PoS* **ICRC**, 921 (2017) [arXiv:1709.01483 [astro-ph.IM]].

[39] H.E.S.S. Collab., *Phys. Rev. Lett.* **117**, 111301 (2017) [arXiv:1607.08142 [astro-ph.HE]].

[40] P.A.R. Ade *et al.* [Planck Collab.], *Astron. Astrophys.* **594**, A13 (2016) [arXiv:1502.01589 [astro-ph.CO]].

[41] Cherenkov Telescope Array Consortium, *Science with the Cherenkov Telescope Array, World Scientific*, DOI:10.1142/10986 [arXiv:1709.07997 [astro-ph.IM]].